

Original Research

# Effects of Tolerance-Induced Preconditioning on Mitochondrial Biogenesis in Undifferentiated and Differentiated Neuronal Cells

Jagdeep K. Sandhu<sup>1,2,\*</sup>, Caroline Sodja<sup>1</sup>, Maria Ribecco-Lutkiewicz<sup>1</sup>, Yu-Ting Wu<sup>3</sup>, Yi-Shing Ma<sup>3</sup>, Yau-Huei Wei<sup>3,4,\*</sup>, Marianna Sikorska<sup>5</sup>

<sup>1</sup>Translational Bioscience, Human Health Therapeutics Research Centre, National Research Council Canada, Ottawa, ON K1A 0R6, Canada

<sup>2</sup>Department of Biochemistry, Microbiology and Immunology, University of Ottawa, Ottawa, ON K1H 8M5, Canada

<sup>3</sup>Center for Mitochondrial Medicine and Free Radical Research, Changhua Christian Hospital, 50046 Changhua, Taiwan

<sup>4</sup>Institute of Clinical Medicine, School of Medicine, National Yang Ming Chiao Tung University, 11221 Taipei, Taiwan

<sup>5</sup>Researcher Emeritus, Human Health Therapeutics Centre, National Research Council Canada, Ottawa, ON K1A 0R6, Canada

\*Correspondence: [jagdeep.sandhu@nrc-cnrc.gc.ca](mailto:jagdeep.sandhu@nrc-cnrc.gc.ca) (Jagdeep K. Sandhu); [yhweibabi@gmail.com](mailto:yhweibabi@gmail.com) (Yau-Huei Wei)

Academic Editor: Josef Jampilek

Submitted: 18 January 2022 Revised: 2 March 2022 Accepted: 4 March 2022 Published: 1 April 2022

## Abstract

**Background:** Mitochondrial biogenesis occurs in response to chronic stresses as an adaptation to the increased energy demands and often renders cells more refractive to subsequent injuries which is referred to as preconditioning. This phenomenon is observed in several non-neuronal cell types, but it is not yet fully established in neurons, although it is fundamentally important for neuroprotection and could be exploited for therapeutic purposes. **Methods:** This study was designed to examine whether the preconditioning treatment with hypoxia or nitric oxide could trigger biogenesis in undifferentiated and differentiated neuronal cells (rat PC12 and human NT2 cells) as well as in primary mouse cortical neurons. **Results:** The results showed that both preconditioning paradigms induced mitochondrial biogenesis in undifferentiated cell lines, as indicated by an increase of mitochondrial mass (measured by flow cytometry of NAO fluorescence) and increased expression of genes required for mitochondrial biogenesis (*Nrf1*, *Nrf2*, *Tfam*, *Nfkb1*) and function (*Cox3*, *Hk1*). All these changes translated into an increase in the organelle copy number from an average of 20–40 to 40–60 mitochondria per cell. The preconditioning treatments also rendered the cells significantly less sensitive to the subsequent oxidative stress challenge brought about by oxygen/glucose deprivation, consistent with their improved cellular energy status. Mitochondrial biogenesis was abolished when preconditioning treatments were performed in the presence of antioxidants (vitamin E or CoQ<sub>10</sub>), indicating clearly that ROS-signaling pathway(s) played a critical role in the induction of this phenomenon in undifferentiated cells. However, mitochondrial biogenesis could not be re-initiated by preconditioning treatments in any of the post-mitotic neuronal cells tested, i.e., neither rat PC12 cells differentiated with NGF, human NT2 cells differentiated with retinoic acid nor mouse primary cortical neurons. Instead, differentiated neurons had a much higher organelle copy number per cell than their undifferentiated counterparts (100–130 mitochondria per neuron vs. 20–40 in proliferating cells), and this feature was not altered by preconditioning. **Conclusions:** Our study demonstrates that mitochondrial biogenesis occurred during the differentiation process resulting in more beneficial energy status and improved tolerance to oxidative stress in neurons, putting in doubt whether additional enhancement of this phenomenon could be achieved and successfully exploited as a way for better neuroprotection.

**Keywords:** oxidative stress; rat PC12 cells; human NT2 cells; differentiation; antioxidant; coenzyme Q<sub>10</sub>; neuroprotection

## 1. Introduction

Cells regulate their energy production, which is mainly carried out by the mitochondrial oxidative phosphorylation system (OXPHOS), according to their needs. Depending on the challenge, mitochondria respond to the energy demands by either subtle change in the activities of OXPHOS enzymes, by changing the expression of enzyme subunits or by increasing the number and size of the organelle, i.e., by biogenesis. For example, mitochondrial proliferation occurs in skeletal muscles in response to the increased contractile activity [1], in adipose tissue in response to adaptive thermogenesis [2], in cardiac myocytes in response to electrical stimulation [3] or hypothermia [4]. Mitochondrial biogenesis is also observed in human en-

dothelial cells in response to hypoxic stimulation *via* vascular endothelial growth factor-Akt-dependent signaling [5], and in human HeLa cells in response to oxidative stress [6]. In clinical settings, the proliferation of abnormal mitochondria was observed in skeletal muscles of patients carrying defective OXPHOS due to the abnormalities of the mitochondrial genome [7]. This implies that reactive oxygen species (ROS), generated either exogenously or endogenously by the respiratory enzymes, might play a role in mitochondrial biogenesis.

Numerous studies, carried out in both heart and brain, revealed remarkable abilities of these tissues to adapt to stress, a phenomenon known as preconditioning, whereby a sublethal dose of stress induces the tolerance to the subsequent lethal insults [8]. A variety



of preconditioning stimuli, including brief periods of ischemia, anoxia, hypothermia and pharmacological agents known to impair mitochondrial function, i.e., iodoacetate (inhibitor of glyceraldehyde-3-dehydrogenase), 3-nitropropionic acid (inhibitor of succinic dehydrogenase) and diazoxide (a selective opener of ATP-sensitive mitochondrial  $K^+$  channel), have been shown to be effective in inducing preconditioning-mediated cytoprotection [9]. In most of these cases the process requires several days to develop and it is governed by the changes in gene expression [10]. The molecular mechanisms by which these stimuli induce the tolerance are not fully understood. Since the same factors known to trigger biogenesis are also capable of inducing cytoprotection in the preconditioning paradigms, we hypothesized that enhanced mitochondrial biogenesis might play a role in neuroprotection.

We asked whether preconditioning treatments, such as hypoxia and nitric oxide (NO), could evoke the same response, i.e., trigger mitochondrial biogenesis and increase tolerance to injuries, in undifferentiated and differentiated post-mitotic neuronal cells. The answer to this question bears relevance to designing better neuroprotective strategies. We utilized two different immortalized neuronal cell lines (rat pheochromocytoma PC12 and human teratocarcinoma NT2 cells) and applied well-established differentiation protocols induced by nerve growth factor (NGF) and all-*trans*-retinoic acid (RA), respectively, to generate terminally differentiated post-mitotic neurons that were arrested in the G0 state. Rat PC12 cells were derived from adrenal medulla and contains neuroblastic cells originating from the neural crest [11]. Upon exposure to NGF, PC12 cells can be differentiated into neuron-like cells with long processes (neuritic varicosities) containing neurosecretory vesicles; hence, these cells have been frequently used to study neuronal differentiation [12]. Human NT2 cells were originally isolated from lung metastasis of primary embryonal carcinoma of the testis. The tumor was xenografted onto a mouse from which the NTERA-2 cells, characteristic of a committed neuronal progenitor cell type, were obtained. These cells can be readily differentiated by treatment with RA into postmitotic neuron-like cells (NT2-N) of the central nervous system [13,14]. The NT2 cells have been utilized in many studies related to neurogenesis, neurotoxicity and neuroprotection [13–15]. Due to their irreversible commitment to a stable neuronal phenotype, the NT2-N cells have also been tested in transplantation studies aimed to repair brain damage [16].

In this study, we used undifferentiated and NGF-differentiated rat PC12 cells, RA-differentiated human NT2-N and primary mouse cortical neurons to study the effects of preconditioning, induced by hypoxia and NO, on mitochondrial biogenesis. The results showed that undifferentiated PC12 cells responded to the preconditioning treatments by increasing mitochondrial copy number per cell and better tolerance to the subsequent oxidative

stress, but the differentiated post-mitotic neurons did not engage mitochondrial biogenesis during such preconditioning treatments. However, mitochondrial biogenesis was taking place in both cell lines during their differentiation and transition to the post-mitotic state. Consistently, post-mitotic neurons had higher mitochondrial copy numbers per cell, higher steady-state levels of ATP and better tolerance to oxidative stress than their undifferentiated counterparts. To our knowledge this is the first comprehensive study that compared the mitochondrial biogenesis response and tolerance to oxidative stress in undifferentiated and differentiated neuronal cells subjected to the same preconditioning treatments.

## 2. Materials and Methods

### 2.1 Cell Cultures

#### 2.1.1 Rat Pheochromocytoma PC12 Cell Culture

PC12 cells were purchased from American Type Culture Collection (ATCC). The cells were plated at a density of  $1 \times 10^5$  cells/well in 12-well plates coated with poly-D-lysine and grown in Dulbecco's modified Eagle's medium (DMEM, cat# 11965-092) supplemented with 10% horse serum and 5% fetal bovine serum (FBS, Wisent Inc., St. Bruno, QC, Canada). Differentiation of PC12 cells was achieved by plating cells on poly-D-lysine (Sigma, cat# P7820) and collagen (BD Biosciences, cat# 354236) coated dishes and grown in DMEM containing 0.5% horse serum in the presence of 50 ng/mL NGF (Alomone Labs, USA). Cells were fed with the fresh medium containing NGF every two days for 7 days.

#### 2.1.2 Human NT2 Cell Culture

NT2/D1 progenitor cells (Stratagene, La Jolla, CA, USA) were cultured in high glucose Dulbecco's modified Eagle's medium (HG/DMEM, cat# 11965-092) supplemented with 10% FBS. Cells were seeded at a density of  $2 \times 10^6$  cells per T75-cm<sup>2</sup> flask and treated three times per week with 10  $\mu$ M RA (Sigma-Aldrich, Oakville, ON, Canada) for 4 weeks. Cells were then harvested by trypsinization and transferred to T175-flasks and cultured for 24–48 hr in HG/DMEM supplemented with 5% FBS in the absence of RA. These cultures consisted of a mixed population of NT2 neuron-like cells (NT2-N) and astrocyte-like cells (NT2-A). Cultures were fed twice a week for 10 days with HG/DMEM supplemented with DNA synthesis inhibitors [1  $\mu$ M 1- $\beta$ -D-arabinofuranosylectosine, 10  $\mu$ M 5-fluoro-2'-deoxyuridine and 10  $\mu$ M uridine (all from Sigma-Aldrich)] to inhibit astrocytic proliferation. Enriched NT2-N cultures were prepared as described previously [13,14]. Briefly, NT2-N cells were collected from mixed cultures 10 days after RA treatment using 0.015% trypsin/EDTA and seeded in 12-well dishes ( $5 \times 10^5$  cells/well) coated with 10  $\mu$ g/mL poly-D-lysine and Matrigel (Collaborative Biomedical Products, Bedford, MA, USA). NT2-N cells were fed with the conditioned medium obtained from 4-week old

NT2-A astrocyte cultures and allowed to mature for another 10–12 days before experiment.

### 2.1.3 Mouse Cortical Neuronal Culture

Primary cultures of mouse cortical neurons were prepared from CD1 mice (Charles River, St. Constant, QC, Canada) in accordance with Canadian Council on Animal Care and the procedures approved by the Institutional Animal Care Committee. Briefly, CD1 mice (postnatal day 3) were sacrificed by CO<sub>2</sub> inhalation, brains were aseptically removed and transferred to 6-cm plates containing calcium- and magnesium-free Hank's balanced salt solution (HBSS, Invitrogen, Burlington, ON, Canada). Under a dissecting microscope, meninges were completely removed, cortices were isolated and transferred to 6-cm dishes containing DMEM supplemented with 10% FBS. Brain tissue was mechanically dissociated into single cells and cell viability was determined using trypan blue exclusion. Approximately  $1 \times 10^5$  cells/mL were seeded in 12-well poly-L-lysine coated plates and incubated at 37 °C for 6 hr. Cultures were examined under a microscope and medium was replenished with fresh DMEM containing 10% FBS. After 48 hr of incubation, cortical neurons were generated by reducing the serum concentration to 0.5% FBS and adding 1  $\mu$ M 1- $\beta$ -D-arabinofuranosylcytosine (Sigma-Aldrich Chemical Co., Oakville, ON, Canada) to limit the proliferation of astrocytes. Cortical neuronal cultures were used for experiments after 2 weeks of *in vitro* growth.

## 2.2 Experimental Treatments

### 2.2.1 Hypoxic Preconditioning

The cells were plated and grown in complete medium for 24 hr under normoxic conditions. For hypoxic preconditioning (HP), cells were incubated for 24 hr at 37 °C in a GasPak 100 chamber containing GasPak Plus gas generator envelopes (BD Biosciences, Franklin Lakes, NJ, USA). The generator envelopes catalytically reduce the oxygen concentration to <1% within 1.0 hr while providing a humidified atmosphere with 5% CO<sub>2</sub> as per manufacturer's information. The generator envelopes contained methylene blue indicator that turns colorless in the absence of oxygen, confirming the generation of an anaerobic environment inside the chamber. The cells were removed from the chamber, placed under normoxia and allowed to recover for 72 hr.

### 2.2.2 Nitric Oxide Preconditioning

For nitric oxide (NO) preconditioning (NP), cells were treated for 6 days with 50  $\mu$ M DETA/NO (diethylene triamine/nitric oxide adduct) added fresh daily. DETA/NO is a NO donor that spontaneously dissociates with a half-life of 20 hr at 37 °C, pH 7.4 to liberate 2 moles of NO per mole of the parent compound [17].

In some experiments, the preconditioning was performed in the presence of antioxidants: PTS (polyoxyethanyl  $\alpha$ -tocopheryl sebacate, the prodrug of vitamin E) at 30  $\mu$ g/mL or Ubisol-Q<sub>10</sub> (containing 10  $\mu$ g CoQ<sub>10</sub> and 30  $\mu$ g PTS/mL) [18,19]. At the end of preconditioning treatment, the antioxidants were removed by washing the cells twice with PBS and replenishing with fresh DMEM medium.

### 2.2.3 Oxygen and Glucose Deprivation

For the induction of oxygen and glucose deprivation (OGD), cells were washed with PBS and switched to DMEM without glucose and supplemented with 10% horse serum and 5% FBS and incubated in the GasPak chamber for 16 hr as described above. The cells were then cultured again in the growth medium for 24 hr before subsequent analysis.

## 2.3 Analytical Methods

### 2.3.1 Cell Viability

The CFDA (5-carboxyfluorescein diacetate) assay was used to measure cell viability as described previously [14,20]. CFDA is a cell-permeant dye that can be taken up by live cells. Once inside the cells, hydrolysis by non-specific esterases results in the formation of a highly charged and fluorescent compound that leaks out of the cells slowly. Cells were incubated with 2.5  $\mu$ g/mL CFDA (Molecular Probes, Eugene, OR, USA) in Earle's Balanced Salt Solution (Sigma-Aldrich, St. Louis, MO, USA) at 37 °C for 30 min and fluorescence was quantified using a CytoFluor™ 2300/2350 system (Millipore, MA, USA) with  $\lambda_{ex} = 480 \pm 20$  nm and  $\lambda_{em} = 530 \pm 25$  nm. Alternatively, cell viability was assessed by staining with Hoechst 33258, a DNA labeling dye. Briefly, cells were grown on poly-D-lysine-coated glass coverslips in 12-well plates and treated as described above. The cells were fixed with 3% paraformaldehyde, washed and mounted in the DAKO mounting medium (DAKO Diagnostics Canada Inc., Burlington, ON, Canada) spiked with 5  $\mu$ g/mL Hoechst 33258 and observed under a Carl Zeiss Axiovert 200M microscope. Approximately 300 cells were counted in three randomly selected fields, and the percentage of cells with condensed and shrunken nuclei were scored as apoptotic cells [14].

### 2.3.2 Flow Cytometry

Cells were harvested by trypsinization, resuspended in PBS with 1% BSA and 50 ng/mL 10-nonyl acridine orange (NAO, Molecular Probes), and incubated at 37 °C for 10 min. NAO was excited at 488 nm and the emitted fluorescence was analyzed at 525 nm using a Coulter Elite ESP flow cytometer (Beckman Coulter, Brea, CA, USA) and EXPO32™ software version 1.0 (Applied Cytometry Systems, Sheffield, UK).

**Table 1. Gene-specific oligonucleotide sequences of the rat primers used for qPCR.**

Gene	Forward primer (5' to 3')	Reverse primer (5' to 3')
<i>Tfam</i>	TCATGACGAGTTCTGCCGTTT	AACAATTCACCACTGCATGCA
<i>Nfkb1</i>	GAAATTCCTGATCCCGACAAGA	TGTTCAATATCCCCAGACCTAACTT
<i>Hif1-<math>\alpha</math></i>	ACACGAGCTGCCTCTTCGA	CAGCCGCTGGAGCTAGCA
<i>Nrf1</i>	GCTCAGCTTCGGGCATTAT	TCCCCAGCCTGGTTTTTC
<i>Nrf2</i>	TCCGAGCCGGTGTAAGTAGAGAT	TACTGGCATGGCCCTCAGAA
<i>Cox3</i>	ACGAGATATCATCCGTGAAGGAA	TTCCGTATCGGAGGCCTTTT
<i>Hk1</i>	CTCGCCTGGACCCCTAATC	TTCACTCATGGGCAATGCAT

Abbreviations of genes: *Tfam*, mitochondrial transcription factor A; *Nfkb1*, nuclear factor kappa B1; *Hif1- $\alpha$* , hypoxia inducible factor 1 subunit alpha; *Nrf1*, nuclear respiratory factor 1; *Nrf2*, nuclear respiratory factor 2; *Cox3*, cytochrome *c* oxidase subunit 3; *Hk1*, hexokinase 1.

### 2.3.3 ATP Content

Cells were harvested in Tris-acetate buffer (pH 7.75) and the ATP content was analyzed using the luciferase-luciferin solution (Thermo Labsystems, Helsinki, Finland) as described previously [20]. The intensity of the emitted light was measured using a Fluostar optima plate reader (BMG Lab Technologies, Germany). ATP concentration was determined from a standard curve ranging from 10–100 pmole ATP. Protein content was determined with the bicinchoninic acid assay (Pierce Chemical Co., TX, USA).

### 2.3.4 Real-Time Quantitative PCR

Total cellular RNA was extracted using TriZol (Molecular Research Center, Inc., Cincinnati, OH, USA) according to the manufacturer's instructions. The extracted RNA was treated with DNase I (Ambion DNA-free DNA removal kit, Invitrogen, Waltham, MA, USA) for 20 min at 37 °C. RNA was reverse transcribed using Superscript II Reverse Transcriptase (Invitrogen, Burlington, ON, Canada). The RNA templates were hydrolyzed in 0.5 N NaOH solution at 65 °C for 20 min. The cDNA was further purified using a QIAquick PCR purification kit (Qiagen Mississauga, ON, Canada) and quantified using the OliGreen ssDNA Quantitation Kit (Invitrogen, Burlington, ON, Canada). Equal amounts of cDNA (2.5 ng each) per sample, in triplicate, were used for real-time PCR, performed by using primers specific for the mitochondrial biogenesis genes (Table 1) and the QuantiTect SYBR Green quantitative PCR Kit (Qiagen, Mississauga, ON, Canada) in the ABI PRISM® 7000 Sequence Detection System (Applied Biosystems, Foster City, CA, USA). Fluorescent products were detected using a GeneAmp 5700 Sequence Detection System (PE Applied Biosystems, Foster City, CA, USA).

### 2.3.5 Transmission Electron Microscopy

Cells were processed for transmission electron microscopy (TEM) as described previously [20,21]. Briefly, cells were fixed with 2.5% (v/v) glutaraldehyde in 100 mM sodium phosphate (pH 7.4), centrifuged and embedded in

22% (w/v) BSA. After washing with 100 mM sodium cacodylate (pH 7.2), the cells were post-fixed with 1% osmium tetroxide in 100 mM sodium cacodylate (pH 7.2) for 1 hr at 4 °C. Cell pellets were stained en bloc with 2% (v/v) aqueous uranyl acetate, dehydrated in ethanol and acetone and then embedded in Spurr epoxy resin. PC12 cells were grown on glass coverslips and differentiated into neuronal cells by treatment with 50 ng/mL NGF. NT2 cells were differentiated into NT2-N with 10  $\mu$ M RA and seeded on glass coverslips coated with poly-D-lysine and Matrigel. After the completion of experiments, all samples were processed for TEM as described above. Ultrathin sections were cut and stained with lead citrate and images were digitally captured on a JEOL 1230 transmission electron microscope (JEOL Ltd., Tokyo, Japan) using the ATM imaging software.

### 2.3.6 Quantification of Mitochondria in TEM Micrographs

The number of mitochondria per cell was counted in at least 25–50 cells in each group of undifferentiated and differentiated PC12 or NT2 cells subjected to preconditioning paradigms (hypoxia and NO treatments). Each count was verified by at least 2 observers blinded to the experimental treatments.

## 2.4 Data Analysis

All results are presented as the mean  $\pm$  SEM of data obtained from 3–4 separate experiments carried out in triplicate, except for the primary mouse neuron experiments where data was obtained from 2 separate experiments performed in duplicate. Differences between two groups were analyzed by unpaired Student's *t*-test. Differences between three or more groups were analyzed by one-way analysis of variance (ANOVA), followed by Dunnett's, Newman-Keuls or Bonferroni's multiple-comparison *post-hoc* tests in GraphPad Prism version 5.02 (GraphPad Software, San Diego, CA, USA). A value of  $p < 0.05$  (\*) is considered as statistically significant and  $p < 0.01$  (\*\*or \*\*\*) and  $p < 0.001$  (\*\*\*) as highly significant.



### 3. Results

#### 3.1 Cytostatic Effects of Preconditioning Treatments

Two experimental preconditioning paradigms (hypoxia and NO treatment) were standardized on undifferentiated PC12 cells to make sure that the applied conditions did not trigger cell death, and ensured cell survival. The hypoxic preconditioning was achieved by placing cells in an anoxic chamber for 24 hr and subsequently allowing them to recover for 72 hr under normal tissue culture conditions. For NO preconditioning we treated cells with DETA/NO, a NO donor, known to spontaneously dissociate and liberate 2 moles of NO per mole of the parent compound [17]. This treatment required 50  $\mu$ M DETA/NO supplied daily for 6 days. Both preconditioning paradigms resulted in a statistically significant reduction in cell numbers at the end of the treatments in comparison to untreated control cells (Fig. 1B,C,  $p < 0.05$ , unpaired  $t$ -test). As compared to untreated control cells, no increase in the number of cells with shrunken and condensed nuclei was seen following hypoxic or NO preconditioning, possibly due to analysis performed at the end of the treatments. Approximately 3–4% apoptotic cells were seen in treated cells. Consistently, microscopic examination of the preconditioned cell cultures revealed fewer numbers of mitotic figures (Fig. 1A, hypoxic treatment).

#### 3.2 Effects of Preconditioning Treatments on Mitochondrial Biogenesis

Highly aerobic tissues, such as the heart, are known to adapt to hypoxia by increasing mitochondrial mass and therefore respiratory capacity [22]. We stained the preconditioned PC12 cells with a fluorescent dye 10-nonyl acridine orange (NAO), known to bind to mitochondria-specific cardiolipin, which is widely used as a marker of mitochondrial mass in living cells. The cell samples were analyzed for NAO staining by flow cytometry (Fig. 2). In the hypoxic preconditioning, a time-dependent elevation of the NAO signal was observed during the 72 hr post-anoxia recovery period (Fig. 2A–C, grey vs. black histograms). Similar results were seen in cells exposed to NO preconditioning (Fig. 2D, grey vs. black histogram). The NAO staining signal increased by ~15% in the hypoxia-treated cells and by ~30% in response to the NO preconditioning (Fig. 2E,  $p < 0.001$ , Dunnett's multiple-comparison test). Thus, both treatments resulted in a higher NAO signal, indicating increased mitochondrial mass, possibly due to enhanced mitochondrial biogenesis.

Mitochondrial biogenesis is a highly regulated process requiring a coordinated transcription of several genes in the nucleus as well as in the mitochondria [23]. Here we were presented with a question whether the above observed changes in the mitochondrial mass could be linked to the relevant changes in gene expression. Accordingly, we evaluated the mRNA expression levels of key transcription factors known to participate in the regulation of mitochon-

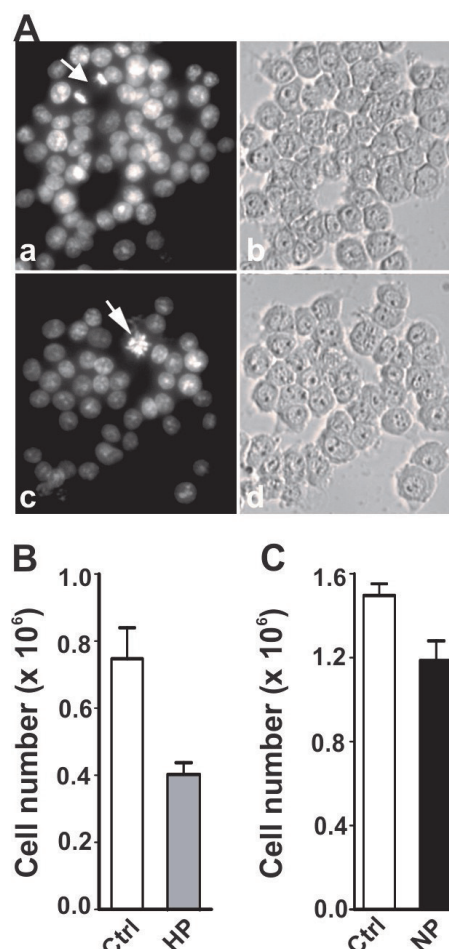


**Fig. 1. Cytostatic effects of preconditioning paradigms.** PC12 cells were incubated for 24 hr in a chamber containing GasPak Plus envelopes followed by a 72 hr recovery under normal culture conditions (A,B; HP) or were treated for 6 days with 50  $\mu$ M DETA/NO (C; NP) as described in the Materials and Methods section. (A) Microscopic evaluation of PC12 cultures. Cells were stained with Hoechst 33258 and imaged on a Zeiss Axiovert microscope. Shown are Hoechst (a,c) and phase contrast (b,d) images of control cells (a,b) and hypoxia preconditioned cells (c,d). Arrows indicate mitotic figures. Magnifications 200 $\times$ . (B,C) Quantitative cell counts of hypoxia (B) and DETA/NO (C) preconditioned cultures. Cells were harvested by trypsinization and the cell numbers were determined using a haemocytometer and trypan blue exclusion method. Shown are cell counts represented as mean  $\pm$  SEM from three experiments from control untreated cultures (Ctrl; white), hypoxia preconditioned (HP; grey) and NO preconditioned cultures (NP; black).

drial biogenesis, such as nuclear respiratory factors NRF-1 and NRF-2, mitochondrial transcription factor A (Tfam), oxidative stress response proteins NF- $\kappa$ B and HIF1- $\alpha$  and two enzyme proteins, hexokinase I (HK1) and cytochrome *c* oxidase subunit 3 (COX3), which are encoded by nuclear and mitochondrial genomes, respectively, in PC12

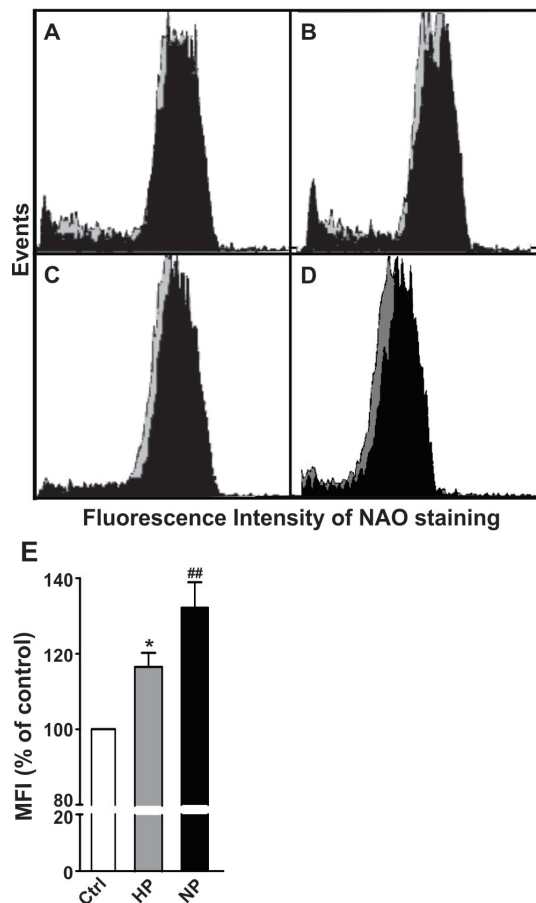


**Fig. 2. Changes in mitochondrial mass in response to the preconditioning treatments.** PC12 cells were either subjected to hypoxia or DETA/NO preconditioning as described in the Materials and Methods. The cells were stained with NAO (50 ng/mL) and analyzed by flow cytometry using a Coulter Elite ESP flow cytometer and EXPO32™ software. Shown in A–C are overlay histograms of NAO fluorescence for control (grey peaks) and hypoxia preconditioned (black peaks) PC12 cells. Cells were analyzed following recovery under normoxic conditions for 24 hr (A), 48 hr (B), and 72 hr (C), respectively. Shown in D is the overlay histograms of NAO fluorescence for control (grey peak) and 6-day DETA/NO preconditioned PC12 cells (black peak). The bar graph in E shows quantification of NAO fluorescence in preconditioned cells. The increases in NAO mean fluorescence intensity (MFI) values in hypoxia preconditioned (HP; grey), NO preconditioned (NP; black) PC12 cells are expressed as percentages of controls (Ctrl; white). Bars show mean  $\pm$  SEM from three separate experiments performed in duplicate.

cells subjected to both preconditioning paradigms (Fig. 3). The results showed that by the end of 24 hr hypoxic treatment the mRNA expression levels of all examined transcription factors were significantly increased in comparison to the untreated control cells, i.e., *Nrf1* and *Nrf2* by ~40–50%, *Hif1- $\alpha$*  ~60%, *Tfam* ~80%, and *Nf $\kappa$ b1* ~400%. The mRNA expression levels of the genes *Cox3* and *Hkl1*

were also elevated by ~40% and 100%, respectively, at the end of the hypoxia (Fig. 3A). The observed changes were transient as the mRNA expression levels of all these genes returned to baseline levels during the subsequent 72 hr recovery phase (data not shown). Similarly, transient changes in the mRNA expression levels of the analyzed genes were observed during DETA/NO preconditioning (Fig. 3B). Significant transient increases in the mRNA expression levels of *Nrf1*, *Nrf2*, *Tfam*, *Nf $\kappa$ b1*, *Hkl1*, and *Cox3* genes were found in cells treated with DETA/NO for 3 days (Fig. 3B; changes ranged between 60% and 120%) with the expression levels returning to the control levels by 6 days of the treatment (data not shown). No change in the mRNA expression level of *Hif1- $\alpha$*  was found here, indicating that the DETA/NO treatment had no effect on the expression of this gene (data not shown).

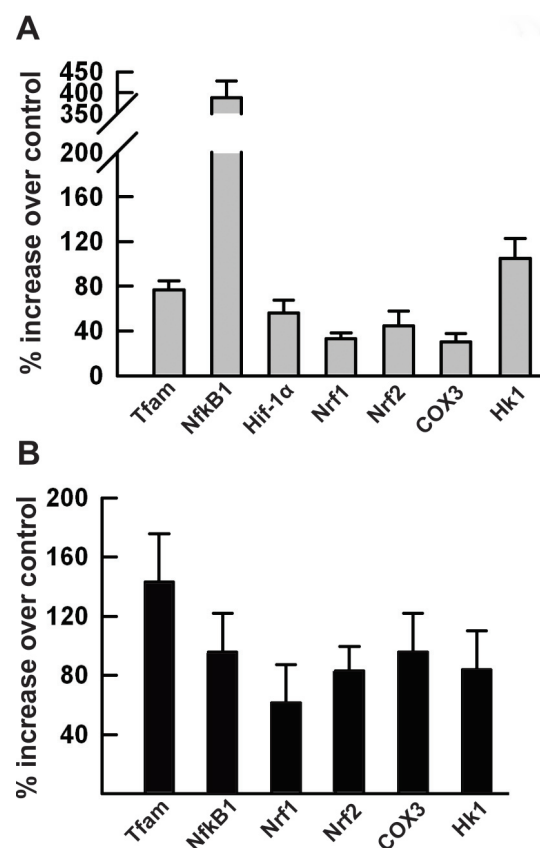


**Fig. 3. Upregulation of mitochondrial biogenesis relevant genes in preconditioned cells.** Total cellular RNA was extracted from 24 hr hypoxia (A) or 72 hr DETA/NO (B) preconditioned PC12 cells. cDNA was synthesized and real time quantitative RT-PCR analysis was performed by using rat gene specific primers (Table 1) as described in the Materials and Methods. The mRNA expression levels of *Nrf1*, *Nrf2*, *Tfam*, *Nf $\kappa$ b1*, *Hkl1*, *Hif1- $\alpha$* , and *Cox3* genes in preconditioned cells were normalized to the controls, and the plotted bars show the mean percent increase  $\pm$  SEM for three separate samples analyzed in triplicate.

Thus, both preconditioning paradigms transiently activated the gene expression of transcription factors NRF1, NRF2 and Tfam as well as the NF- $\kappa$ B signaling pathway, which led to the increased gene expression of metabolic enzymes HK1 and COX3 in undifferentiated PC12 cells. These changes are consistent with the increase of mitochondrial biogenesis induced by preconditioning treatment. No significant differences were observed in the expression levels of peroxisome proliferator-activated receptor  $\gamma$  coactivator-1 $\alpha$  (PGC-1 $\alpha$ ) following hypoxia or NO preconditioning, suggesting that the endogenous stress levels were sufficient to control the process of mitochondrial biogenesis.

Subsequently, we assessed the mitochondrial morphology of the cells by transmission electron microscopy (Fig. 4). The electron micrographs of cells treated with hypoxia (Fig. 4B) as well as DETA/NO (Fig. 4C) revealed dynamic intracellular tubular networks of numerous mitochondria with heterogeneous morphology and clear evidence of fission and fusion (Fig. 4B,C and enlarged insets) of mitochondria that are scattered throughout the cytoplasm. These images were strikingly different from those observed in the untreated control cells (Fig. 4A) in which a smaller number of mitochondria with normal rounded morphology was observed (Fig. 4A–C insets).

### 3.3 Increased Tolerance of Preconditioned Cells to OGD

Preconditioned PC12 cells were challenged with oxygen-glucose deprivation (OGD), a well-established *in vitro* model of ischemia-reperfusion injury of the brain [24]. Morphological examination of Hoechst-stained cultures indicated that cell viability was higher in the preconditioned cells challenged with OGD (Fig. 5A,b, hypoxia; Fig. 5A,d, DETA/NO) than control cells without preconditioning (Fig. 5A,a,c). Whereas cell death was evident in control cultures after 24 hr of OGD (Fig. 5A,a,c, numerous pyknotic nuclei), the preconditioned cell cultures appeared far less affected by OGD (Fig. 5A,b,d, normal diffuse chromatin distribution in the majority of nuclei). CFDA live cell assay confirmed the above observations (Fig. 5B). Approximately 50% of OGD-treated control cells lost viability ( $p < 0.0001$ , Newman Keuls multiple-comparison test), but the hypoxic preconditioning almost significantly attenuated the OGD-induced cell death ( $p < 0.0001$ , Newman Keuls multiple-comparison test). These results were also confirmed by counting the cells stained with trypan blue and Hoechst 33258.

### 3.4 Effect of Antioxidants on Mitochondrial Biogenesis in Undifferentiated Cells

Low levels of ROS act as signaling molecules and stimulate mitochondrial biogenesis in diverse cell types [25]. We then investigated whether intracellularly generated ROS played any role in the observed mitochondrial biogenesis during the preconditioning treatments (Fig. 6).

Accordingly, the preconditioning was performed in the presence of antioxidants, CoQ<sub>10</sub> (Ubisol-Q<sub>10</sub>) or the pro-drug form of  $\alpha$ -tocopherol (PTS), and the changes in mitochondrial mass (NAO staining) were assessed (Fig. 6A). As shown above in Fig. 2, hypoxic preconditioning of undifferentiated PC12 cells resulted in a clear increase in the NAO staining signal; however, when preconditioning was performed in cells in the presence of PTS or Ubisol-Q<sub>10</sub> (formulation of CoQ<sub>10</sub> and PTS) the previous increase in NAO staining was abolished. As summarized in Fig. 6A, the increases in NAO staining generated during either of the two preconditioning (~15% in hypoxia and ~30% in DETA/NO) were not detected in the presence of antioxidants. These findings suggest clearly that ROS acted as a trigger and/or a mediator of the mitochondrial biogenesis induced by preconditioning.

### 3.5 Effects of Preconditioning Treatments on Mitochondrial Biogenesis in Differentiated Neurons

NGF-differentiated PC12 cells [11] and human NT2-derived neurons [13,26] were used in this set of experiments. The differentiated cells expressed neuronal markers,  $\beta$ -III tubulin and microtubule-associated protein (MAP-2) and had exited the cell cycle, confirmed by the absence of Ki67-positive immunoreactivity. These cells were subjected to the same preconditioning treatments (24 hr hypoxia plus 72 hr recovery or 6-day exposure to DETA/NO) and neuronal tolerance to the subsequent OGD treatment was tested. The data obtained for PC12 cells are shown in Fig. 7A. Exposure of PC12 neurons to OGD resulted in nearly 30% loss of cell viability ( $p < 0.05$ ) and neither hypoxia nor NO preconditioning brought about any significant neuroprotection. Similar results were obtained in experiments using NT2 neurons (Fig. 7B).

The PC12- and NT2-derived neurons were also analyzed by NAO staining to establish whether any changes in the neuronal mitochondrial mass occurred after preconditioning. The results showed no increase in NAO fluorescence with respect to controls, neither in hypoxia preconditioned PC12 neurons (Fig. 7C) nor in hypoxia preconditioned NT2 neurons (Fig. 7F), nor in DETA/NO pre-treated neurons (data not shown). These findings indicate that mitochondrial mass was not increased in neurons by these preconditioning treatments.

Analysis of the transcriptional machinery involved in mitochondrial biogenesis by RT-PCR also failed to show any changes in the mRNA levels of the relevant transcription factors (NRF-1, NRF-2, Tfam, NF- $\kappa$ B) in preconditioned neurons in comparison to the controls (data not shown), which support the notion that the preconditioning treatments did not activate mitochondrial biogenesis in differentiated neurons. These findings were further corroborated by electron microscopy (Fig. 7E,H). The micrographs revealed a dense network of heterogeneous mitochondria in cytoplasmic space with numerous events of fission and fu-



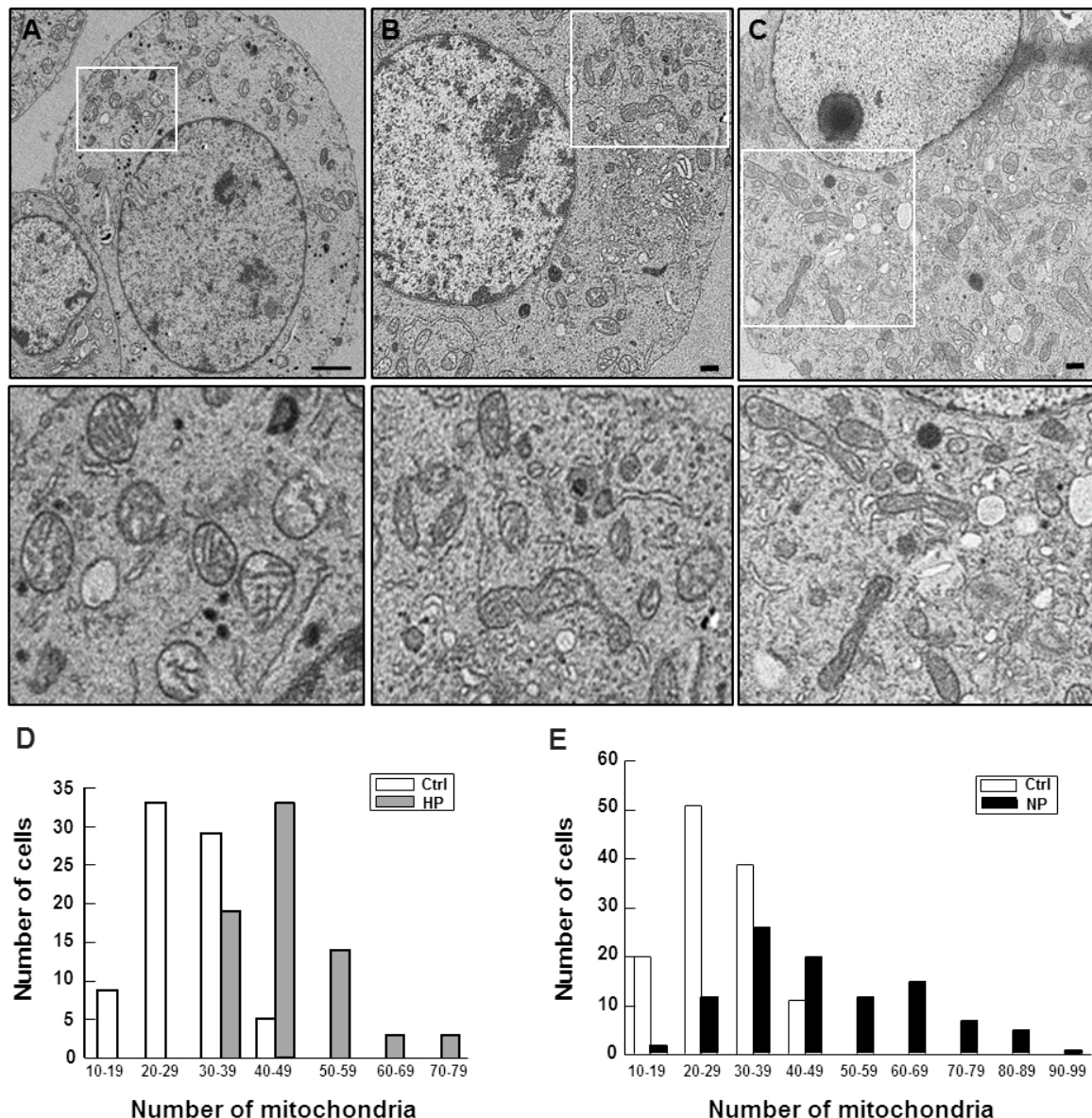


**Fig. 4. Mitochondrial distribution and counts in preconditioned cells.** PC12 cells (control – A; preconditioned B and C) were processed for electron microscopy as described in the Materials and Methods. Ultrathin sections were cut and stained with lead citrate and images were digitally captured on a JEOL 1230 transmission electron microscope. (A–C) Electron micrographs of a typical control PC12 cell (A), a hypoxia preconditioned PC12 cell (B) and a DETA/NO preconditioned PC12 cell (C). TEM images of PC12 cells (scale bar = 2  $\mu$ m). Insets show typical mitochondrial morphologies in the control and preconditioned samples. (D–E) Distribution of mitochondria in PC12 cells. Cell sections with similar cytoplasmic volumes, magnified at 1000 $\times$ , were used for counting of mitochondria. For each experimental condition 80 cells were analyzed. Distribution of mitochondria in hypoxia preconditioned (D) and DETA/NO preconditioned cells (E) are plotted. White bars represent control untreated; grey bars hypoxia indicate preconditioned and black bars DETA/NO preconditioned cell populations. Electron micrographs of cell sections with similar cytoplasmic volumes were used to count the number of mitochondria per cell and, in total, 80 cells per treatment were assessed (Fig. 4D,E). The data indicate a marked increase in the number of mitochondria per cell in both treatments (hypoxia and DETA/NO, Fig. 4D,E, respectively) and a significant shift in distribution towards a higher number of mitochondria per cell. For example, whereas the majority of untreated cells (~80%) contained 20–40 mitochondria/cell, a similar percentage of preconditioned cells contained between 30–60 mitochondria/cell (Fig. 4D,E). Indeed, many preconditioned cells had >50 mitochondria while such high numbers of mitochondria were not seen in the control cells. Thus, consistent with the data presented in Figs. 3,4, mitochondrial biogenesis occurred during the preconditioning of undifferentiated PC12 cells and resulted in significantly higher numbers of mitochondria per cell.



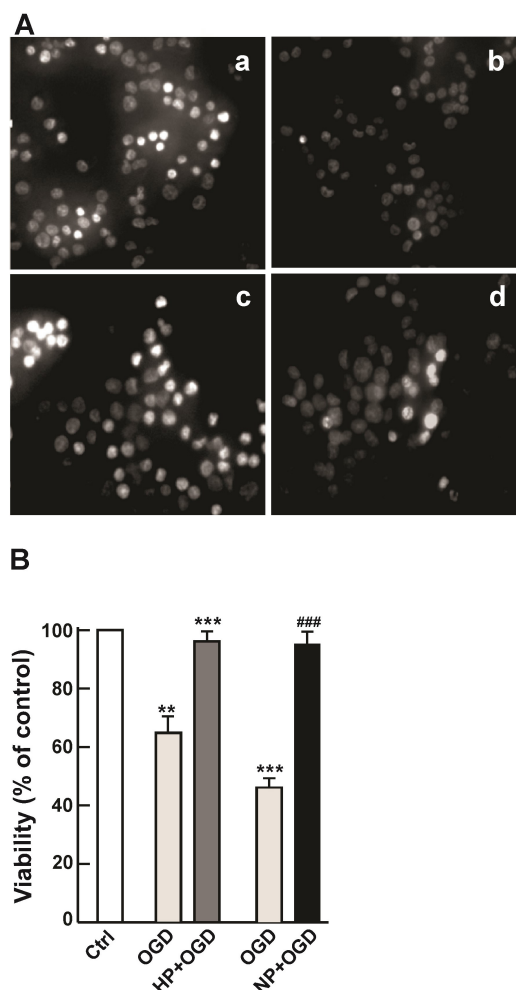


**Fig. 5. Increased tolerance of preconditioned cells to subsequent OGD stress.** PC12 cells, untreated and preconditioned by HP or NP, were subsequently challenged with 16 hr OGD followed by 24 hr of recovery. (A) Microscopic evaluation of PC12 cells challenged with OGD. Cells were stained with Hoechst 33258 and imaged on a Carl Zeiss Axiovert microscope. Shown are untreated control cells (a) and (c), hypoxia preconditioned cells (b) and NO preconditioned cells (d). (B) Cell viability was analyzed by CFDA assay as described in the Materials and Methods. Bars show the mean  $\pm$  SEM of data obtained from three separate experiments.

sion (Fig. 7E,H plus insets). Quantitative analysis of mitochondria did not reveal any differences between preconditioned and control neurons. As shown in Fig. 7D,G similar distributions of mitochondria within the cell populations were seen in PC12 neurons (Fig. 7D) and human NT2-derived (Fig. 7G) neurons regardless whether they were exposed to hypoxia or NO preconditioning. Unexpectedly, differentiated neurons contained a higher number of mitochondria per cell, and between 50 and 100 organelles were counted in each of the great majority of cells (Fig. 7D,G).

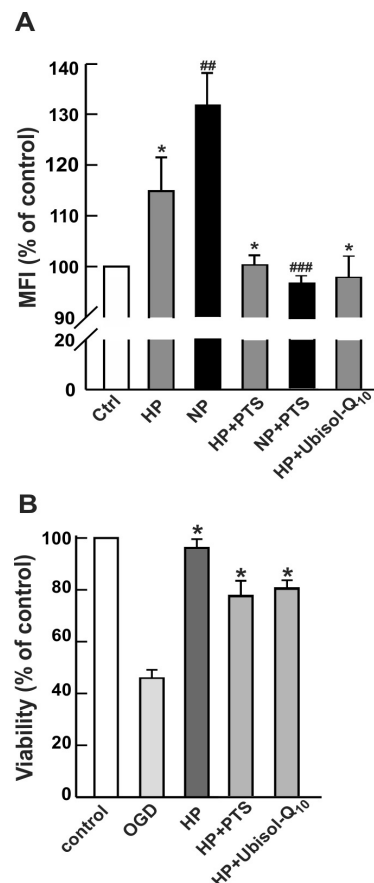


**Fig. 6. Effects of antioxidants on mitochondrial biogenesis and the tolerance of PC12 cells to OGD.** PC12 cells were preconditioned either by hypoxia (HP) or NO (NP) in the absence or presence of antioxidant PTS (water-soluble derivatized vitamin E) or Ubisol-Q<sub>10</sub> (water-soluble CoQ<sub>10</sub>). (A) Preconditioned cells were stained with NAO and analyzed by flow cytometry. Bars show NAO mean fluorescence intensity (MFI) values expressed as percent of untreated control from 3 separate experiments performed in duplicate (mean  $\pm$  SEM). The data are normalized to control values and the bars show the mean  $\pm$  SEM of data from three separate experiments performed in duplicate. White bar, control; grey bars, hypoxia preconditioned cells; black bars, DETA/NO preconditioned cells. The addition of antioxidants is marked as PTS or Ubisol-Q<sub>10</sub>. (B) Cells were subjected to hypoxic preconditioning in the absence or presence of antioxidants (PTS or Ubisol-Q<sub>10</sub>) and subsequently challenged with 16 hr of OGD. Following a recovery of 24 hr, cell viability was analyzed by the CFDA assay as described in the Materials and Methods. Although inclusion of antioxidants (either PTS or Ubisol-Q<sub>10</sub>) during the preconditioning treatments abolished the changes in the mitochondrial mass (Fig. 6A), their presence was evidently cytoprotective against OGD (Fig. 6B,  $p < 0.0001$ , Newman Keuls multiple-comparison test), suggesting the involvement of ROS signaling pathways in this response.

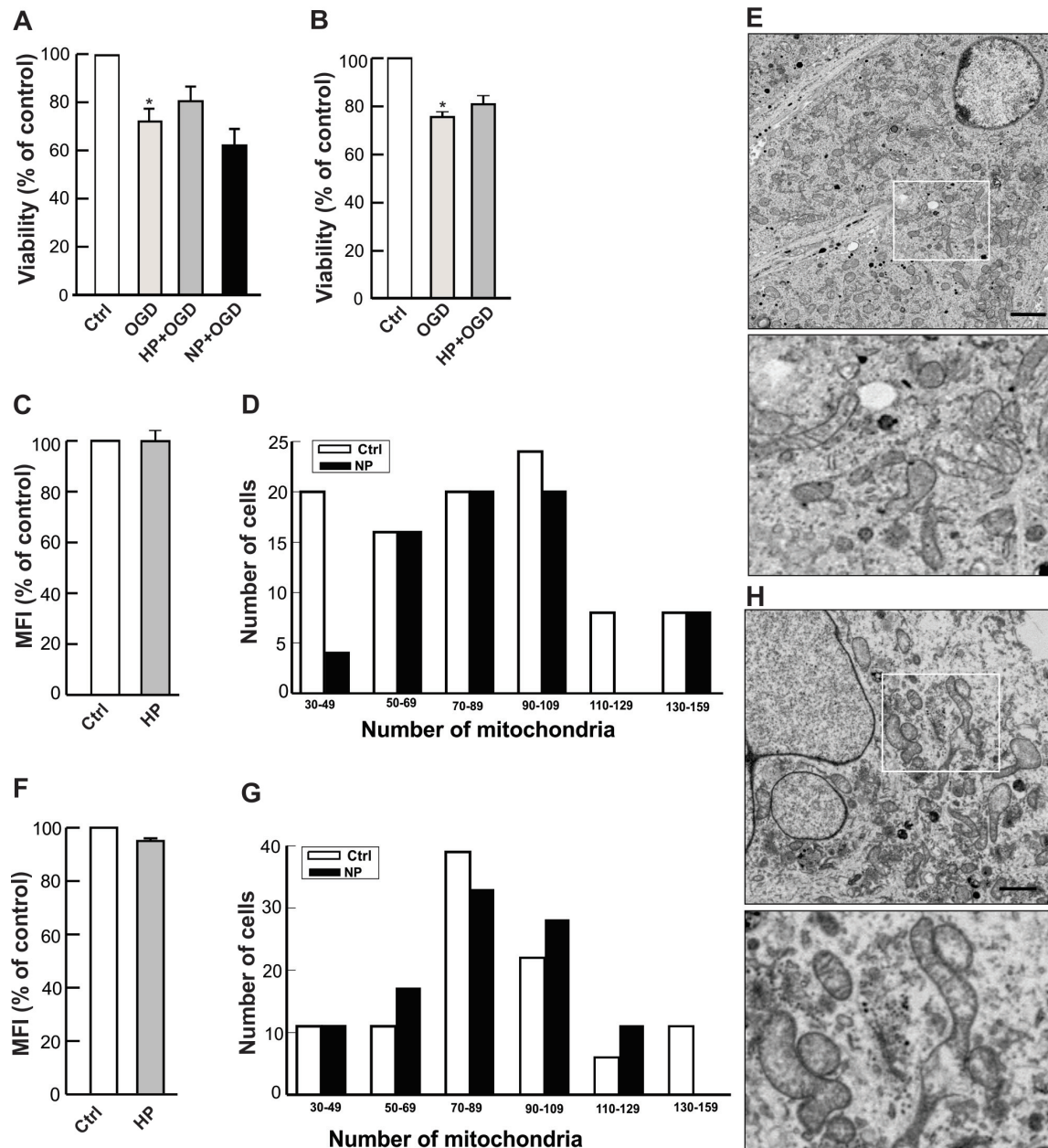


**Fig. 7. Effects of preconditioning on differentiated neuronal cells.** NT2 cells were differentiated by retinoic acid (A,F–H) and PC12 cells by NGF (B,C–E) as described in the Materials and Methods section. (A,B) The differentiated neurons (NT2/N -A and PC12 neurons -B) were subjected to either hypoxia (HP) or NO (NP) preconditioning and were subsequently challenged with 16 hr OGD. Cell viability was analyzed by the CFDA assay as described in the Materials and Methods. Bars show the mean  $\pm$  SEM of data from three separate experiments performed in duplicate. (C,F) The differentiated and preconditioned neurons (C- PC12 neurons; F- NT2/N) were stained with NAO and analyzed by flow cytometry using a Coulter Elite ESP flow cytometer and EXPO32<sup>TM</sup> software. Bars show the percent increase in mean fluorescence intensity over control cells of data of three separate experiments performed in duplicate. (E,H) Electron micrographs of NO (NP) preconditioned PC12 neurons (E and enlarged inset) and NT2/N (H and enlarged inset) cells. Cells were processed for electron microscopy and images were digitally captured on a JEOL 1230 electron microscope as described in the Materials and Methods. Scale bar = 2  $\mu$ m. Shown in D and G is the distribution of mitochondria in untreated vs. DETA/NO (NP) preconditioned PC12 neurons (D) and NT2/N (G) neurons. Cell sections with similar cytoplasmic volumes, magnified at 1000 $\times$ , were used for the counting of mitochondria. For each experimental condition 80 cells were analyzed. White bars represent untreated and black bars indicate preconditioned neuronal cell populations.

### 3.6 Mitochondrial Biogenesis during Neuronal Differentiation

Mitochondrial density is regulated by a continuous cycle of fusion and fission [27]. These events allow the organelle to exchange content such as mtDNA, membranes and various metabolites to maintain a healthy and functional mitochondrion. These events were clearly revealed in the TEM micrographs of cell cross sections (Figs. 4,7). Comparison of electron microscopy images (Fig. 4A–C,7E–H) and quantitative mitochondrial counts (Fig. 4D,E,7D–G) revealed that differentiated neurons contained an increased number of mitochondria per cell than their undifferentiated counterparts, suggesting that mitochondrial biogenesis must have occurred during the neuronal differentiation processes. The data that support this conclusion are presented in Fig. 8. Whereas the great majority of undifferentiated cells (both PC12 and NT2 cells; Fig. 4D,E) contained between 20 and 40 mitochondria, the number of mitochondria in the great majority of neurons reached 70–130 per cell (Fig. 8A). Accordingly, the NAO staining in PC12 neurons, for example, was nearly 2-times higher (Fig. 8B) and a steady-state content of ATP was 50% higher than those of undifferentiated PC12 cells (Fig. 8C). Overall, the differentiated cultures responded much less severely to OGD, with only about 20% cell death 24 hr after the OGD insult (Fig. 7B) as compared to 50% death after OGD for undifferentiated cultures (Fig. 5B). These observations confirmed once again the significant role of mitochondria in maintaining cell viability, especially under oxidative stress.

We also asked whether intracellular ROS signaling was critical for mitochondrial biogenesis during neuronal differentiation. To address this issue, PC12 cells were differentiated by treatment with NGF for 7 days in the absence or presence of Ubisol-Q<sub>10</sub> and the NAO fluorescence intensity was measured. The presence of antioxidants reduced the NAO signal by ~15% suggesting that the quenching of ROS signaling negatively affected mitochondrial biogenesis in these cell cultures (data not shown).

The effects of the preconditioning treatments with hypoxia and NO were also tested in the primary cultures of mouse cortical neurons and the results showed no difference in the mitochondrial mass and neuroprotection against OGD between preconditioned and control cell cultures (Fig. 9). Thus, the above results obtained with differentiated and cultured rat and human neuronal cells *in vitro*, are consistent with the phenomenon observed in the primary culture of mouse cortical neurons *in vivo*.

## 4. Discussion

Mitochondrial biogenesis, which has been observed in various paradigms of experimental preconditioning, is regarded by many as a practical way of enhancing cellular tolerance to injuries; hence, its activation is especially significant in the CNS. However, it is still unclear whether this phenomenon could be easily induced in post-mitotic neu-

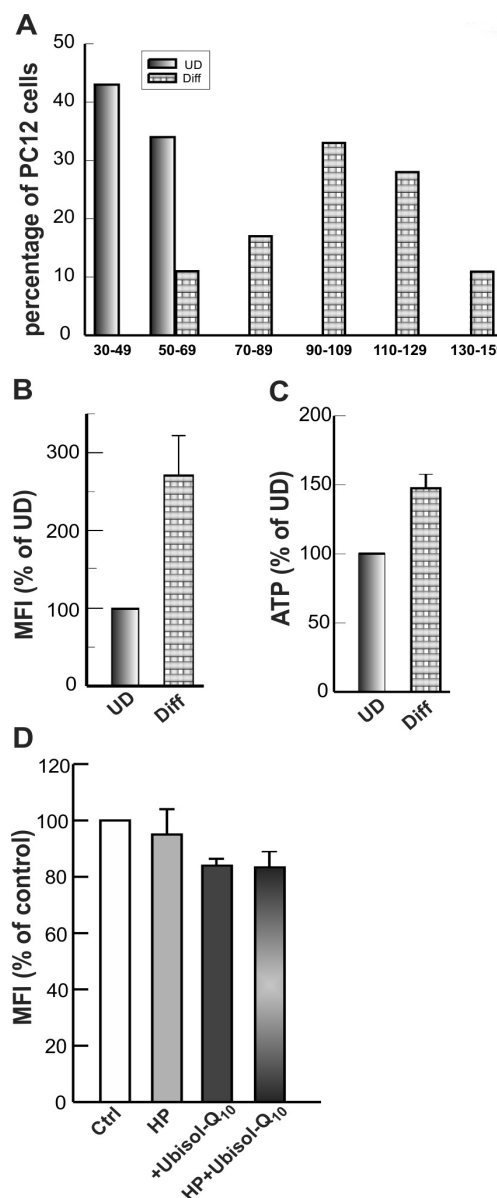


**Fig. 8. Mitochondrial content, energy status during differentiation of PC12 cells.** (A) Undifferentiated and differentiated PC12 cells were fixed, stained, embedded, and sectioned for electron microscopy as described in Materials and Methods. TEM images of cells were digitally captured on a JEOL 1230 electron microscope, and the number of mitochondria per cell slice was determined for cells with similar cytoplasmic volumes. (B) The fluorescence intensity of NAO was analyzed by flow cytometry for undifferentiated (UD) and differentiated (Diff) PC12 cells. (C) Basal ATP levels were measured by the luciferase assay for UD and Diff-PC12 cells. (D) Differentiated PC12 cells were hypoxia preconditioned in the presence or absence of antioxidants and mitochondrial mass was determined by staining with NAO and analysis by flow cytometry. Bars show the percent increase in the mean fluorescence intensity (MFI) values over control cells from three separate experiments.



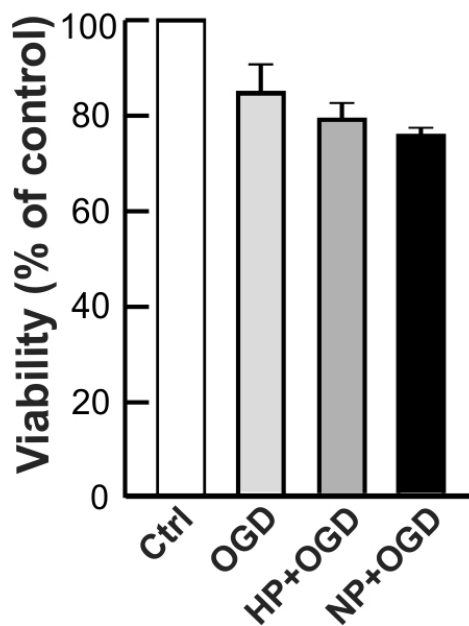


**Fig. 9. Effect of preconditioning on the viability of primary mouse cortical neurons.** Primary mouse cortical neurons were prepared as described in Materials and Methods. Cells were treated with hypoxia for 24 hr followed by 72 hr recovery or with DETA/NO for 6 days. Cell viability was determined using the CFDA assay after a 16 hr OGD followed by 24 hr of recovery. The control group represents cells without preconditioning and OGD challenge. Bars show the mean  $\pm$  SEM of data obtained from 2 separate experiments performed in duplicate.

rons by methods shown to work in proliferating cells. With that in mind, we compared the mitochondrial biogenesis responses to non-lethal preconditioning in undifferentiated neuronal cells and in post-mitotic neurons. To our knowledge, no such direct comparison was previously reported and the data presented here bears relevance to the mechanisms controlling mitochondrial biogenesis and its role in neuroprotection. The preconditioning paradigms, hypoxia and NO treatments, have been extensively tested both *in vitro* and *in vivo* studies and induced tolerance in a variety of cells and tissues [28–32]. In this study, we applied the preconditioning methods that were suitable for *in vitro* treatments of all neuronal cells.

Mitochondria are dynamic organelles that are not synthesized *de novo*, but are formed from pre-existing organelles through fusion and fission. This results in the formation of constantly changing intracellular tubular networks observed in Figs. 4,7. Through mitochondrial fission, smaller mitochondria are created to which new mitochondrial contents created during mitochondrial biogenesis can be added. Mitochondrial biogenesis, in turn, requires the synthesis of new mtDNA, new proteins and membrane components. The observed activation of transcriptional regulatory networks (Fig. 3) clearly indicate that these processes indeed occur during the preconditioning treatments.

We have shown that while undifferentiated PC12 cells responded to the preconditioning treatments (hypoxia and NO) by increasing the mitochondrial number per cell and better tolerance to the subsequent oxidative stress, but the differentiated post-mitotic neurons did not engage mitochondrial biogenesis machinery during such preconditioning treatments. However, mitochondrial biogenesis occurred in both cell lines during their differentiation and transition to the post-mitotic state. Consistently, post-mitotic neurons had higher number of mitochondria per cell, higher steady-state levels of ATP and better tolerance to oxidative stress than their undifferentiated counterparts. To our knowledge this is the first comprehensive study that compared mitochondrial biogenesis response and tolerance to oxidative stress in undifferentiated and differentiated neuronal cells subjected to preconditioning treatments. In a study using clonal cell lines of murine neuroblastoma C1300 cells, mitochondrial biogenesis and the consequent increase in mitochondrial mass were shown to correlate with different stages of neuronal differentiation [33].

It is well established that mitochondrial biogenesis is linked to increased mitochondrial ROS production, which can act as important second messengers and activate the retrograde signaling cascades [34]. Such retrograde signaling, originated from mitochondria, is fundamental to coordinating the transcription of nuclear and mitochondrial genes as required for mitochondrial biogenesis to take place [35]. Although the exact chemical nature of ROS engaged in this phenomenon is unknown, it is plausible that the majority of ROS include superoxide anions produced when unpaired electrons escape from the electron transport chain (primarily at sites of Complexes I and III) during respiration and react with molecular oxygen. Superoxide anions, in turn, can spontaneously or enzymatically be converted to hydrogen peroxide, which can also act as a second messenger [36]. Similar types of ROS are known to be produced during various preconditioning paradigms and elimination of ROS can abolish the observed neuroprotective effects [37,38]. Accordingly, we found that hypoxic and NO preconditioning of PC12 cells in the presence of antioxidants or scavengers of ROS (PTS and Ubiol-Q<sub>10</sub>), the increase in mitochondrial mass was abolished and failed to protect PC12 cells against a subsequent OGD challenge (Fig. 6). Our findings support the notion that ROS and NO are generated during the preconditioning treatments and act as signaling molecules to increase mitochondrial biogenesis and provide neuroprotection against a lethal injury. Additionally, we found increased mRNA expression levels of NF- $\kappa$ B in PC12 cells exposed to hypoxic and NO preconditioning (Fig. 3), suggesting that activation of the gene expression is associated with neuroprotection. Upon activation, NF- $\kappa$ B p65 subunit is translocated from the cytoplasm into the nucleus where it binds to the DNA consensus sequences on various target genes leading to neuroprotection. NF- $\kappa$ B is a well-characterized transcription factor with multifaceted

roles. Increasing evidence points to an active crosstalk between the NRF-2 and NF- $\kappa$ B signaling pathways and both transcription factors bind to the cAMP response element-binding protein (CREB) to provide neuroprotective effects [39]. In line with this, several studies have demonstrated increases in cellular antioxidant defense system including manganese superoxide dismutase, glutathione peroxidase, catalase and Bcl-2 [40] in preconditioned cells. Although increased production of mitochondrial ROS is associated with mitochondrial dysfunction and disease, low levels of ROS generated during normal oxidative metabolism serve as signaling molecules, promotes mitochondrial biogenesis [41] and can be exploited to provide long-lasting neuroprotective effects [42].

Mitochondrial biogenesis is a complex process that is regulated by a highly orchestrated crosstalk between the nuclear and mitochondrial genomes and works in concert with the members of the peroxisome proliferator-activated receptor  $\gamma$  coactivator-1 (PGC-1) family. In undifferentiated PC12 cells subjected to hypoxic and NO preconditioning treatments we found an increase in the expression of the nuclear respiratory factors NRF-1 and NRF-2, which are regulated by PGC-1 $\alpha$ . Their activation is known to drive the transcriptional machinery necessary for the expression of Tfam [34]. Although encoded by nuclear genome, Tfam can be translocated into mitochondria leading to an increase in the transcription of mitochondrial genes that encode mitochondrial proteins. Accordingly, gene expression of mitochondrial proteins COX3 and HK1 (Fig. 3) was upregulated following preconditioning treatments. HK1 is not only involved in the rate limiting step of glycolysis but ~70–90% of HK1 in the brain is associated with the outer mitochondrial membrane [43]. The mitochondrial-bound HK1 has been shown to play an important role in neuronal survival, neurite outgrowth, maintenance of glutathione levels and prevention of apoptosis and oxidative damage. COX3 is one of main transmembrane subunits of cytochrome *c* oxidase, an oligomeric enzymatic complex located in the mitochondrial inner membrane and the mitochondrial hexokinase catalyze the first essential step of glucose metabolism, the conversion of glucose into glucose-6-phosphate [44]. This directly couples extramitochondrial glycolysis to intramitochondrial oxidative phosphorylation. This further supports our conclusion that the tested pre-conditioning paradigms not only led to the increase of the mitochondrial mass, the mitochondrial copy number, but also resulted in the creation of functional organelles.

Although PGC-1 $\alpha$  is known as a “master regulator of mitochondrial biogenesis”, recently the Nrf2 (nuclear factor E2-related factor 2)/ARE (antioxidant response element) signaling cascade has emerged as a novel regulator of mitochondrial biogenesis [45]. Increased production of reactive oxygen and nitrogen species, particularly hydrogen peroxide, results in the translocation of Nrf2 from the cytoplasm into the nucleus where it can interact with PGC-1 $\alpha$  to regu-

late mitochondrial biogenesis. It has been shown that PGC-1 $\alpha$  gene promoter contains two AREs and thereby Nrf2 may directly interact with PGC-1 $\alpha$  [46]. In our study it is possible that the interaction between the Nrf2/ARE and PGC-1 $\alpha$  pathways resulted in increased mitochondrial biogenesis and the observed neuroprotection.

Mitochondrial organogenesis in post-mitotic neurons is not yet fully understood, hence the specific pathways involved in its regulation remain unknown. In our experiments, hypoxic and NO preconditioning of differentiated either PC12, NT2 neurons or primary mouse cortical neurons did not result in the activation of mitochondrial biogenesis processes and did not further protect post-mitotic neurons against cell death inducing signals (Figs. 7,8,9). Interestingly, increased number of elongated tubular mitochondria, suggestive of mitochondrial fission-fusion was observed in differentiated PC12 and NT2 cells (Fig. 7E–H). We observed similar change of morphological features of mitochondria in undifferentiated cells following preconditioning treatments (Fig. 4). Thus, mitochondrial biogenesis clearly occurred during the differentiation processes as evidenced by the number of mitochondria per neuron being higher than the undifferentiated counterparts (Figs. 4,7), which resulted in more beneficial metabolic outcomes, higher steady-state ATP levels, better resistance to cell death-inducing insults (Figs. 7,9).

Since mitochondria cannot be synthesized *de novo*, they are produced from pre-existing mitochondria that are used as a template for mitochondrial biogenesis during cell cycle [47]. Mitochondrial biogenesis is a complex process that is regulated by a highly orchestrated and integrated crosstalk between the nuclear and mitochondrial genomes. This process requires transcription, translation, modification and functional assembly over 1500 proteins, of these only 13 polypeptides are encoded by mtDNA. The vast majority of proteins are transcribed from the nuclear genome and subsequently imported from the cytoplasm into the mitochondria by a highly specialized nanomolecular machinery known as the TOM complex, which is a gateway for almost all mitochondrial proteins [48]. Hence both nuclear and mitochondrial genomes must be transcriptionally and translationally competent and cells must be able to engage all vital activities in the cycling cells. Our findings on undifferentiated neural cells showed clearly that prior to engaging mitochondrial biogenesis processes the proliferating cells entered a temporary cell cycle arrest state and became quiescent (Fig. 1). Typically, quiescent cells can re-enter cell cycle when activated as they did not reach the growth factor dependent restriction points of the G1 phase and their genome remains transcriptionally competent. CDKs (cyclin dependent kinases) in association with CKIs (cyclin regulatory subunits/inhibitors) govern cell cycle progression or arrest. Stimulation of mammalian cells with mitogens or growth factors induces the expression of cyclin D1 resulting in phosphorylation of Rb, weakening its inter-

action with E2F, leading to transcription of genes needed for cells to enter the S-phase. This phenomenon of reversible activation of nuclear gene transcription in cell cycle competent cells might be the reason for observed mitochondrial biogenesis in proliferating cells, but these mechanisms are inactivated in quiescent cells. Besides the classical role of E2F1 in regulating cell cycle from G1-S transition, increasing evidence also implicates E2F1 in the regulation of mitochondrial function through interactions with NRF1 and NRF2, key regulatory factors of mitochondrial biogenesis [49]. E2F1 regulates self-renewal of human induced pluripotent stem cells [50], but in post-mitotic neurons E2F1 acts as a cell cycle suppressor [51], mainly by the ability of E2F1 to bind Rb and block the cells to enter S-phase. Earlier work indicated that injured neurons attempt to re-enter cell cycle by aberrantly activating the expression of cyclin D1 [52–54], leading to a false hope that these events are neuroprotective. Regrettably, these attempts lead to neuronal cell death, not neuroprotection [54].

## 5. Conclusions

In summary, we have demonstrated that although mitochondrial biogenesis could be induced in undifferentiated rat PC12 cells, this phenomenon could not be induced in post-mitotic rat PC12 and human NT2 neuron-like cells as well as in primary mouse cortical neurons using the two preconditioning paradigms employed in this study. Pharmacological induction of mitochondrial biogenesis to restore mitochondrial function and homeostasis remains an attractive therapeutic strategy for the treatment of brain diseases. The US Food and Drug Administration (FDA) has approved many pharmacological agents, such as pioglitazone (thiazolidinedione-type), lasmiditan (5-hydroxytryptamine receptor 1F receptor agonist), and formoterol ( $\beta$ 2-adrenoreceptor agonist), which can induce mitochondrial biogenesis and may be repurposed for the treatment of a variety of CNS disorders [55,56].

## Author Contributions

JKS, Y-HW and MS wrote the grant proposal, designed and managed the research work. CS and MR-L performed the experiments, generated data and contributed to analyses and plotting of the data. JKS and MS composed and wrote the manuscript. Y-HW, Y-TW and Y-SM made constructive changes to the final text of the manuscript and contributed to significant editing of the manuscript. All authors have read and approved the final manuscript.

## Ethics Approval and Consent to Participate

All animal work was performed in accordance with the guidelines provided by the Canadian Council on Animal Care and the procedures approved by the institutional Animal Care Committee at the National Research Council Canada (ACC protocol #2011.10).

## Acknowledgment

The authors are thankful to Erin Twomey, Patricia Lanthier and Roger Tremblay for their excellent technical assistance in carrying out some experiments, as well as Peter Rippstein, University of Ottawa Heart Institute for his help with electron microscopy.

## Funding

This work was supported by a joint collaborative grant from the National Research Council Canada and the National Science Council Taiwan and a grant supported by the Ministry of Science and Technology, Taiwan (MOST 110-2320-B-371-001).

## Conflict of Interest

The authors declare no conflict of interest. Y-HW is serving as the guest editor and editorial board member of this journal. We declare that Y-HW had no involvement in the peer review of this article and has no access to information regarding its peer review. Full responsibility for the editorial process for this article was delegated to JJ.

## References

- [1] Perry CGR, Hawley JA. Molecular basis of exercise-induced skeletal muscle mitochondrial biogenesis: Historical advances, current knowledge, and future challenges. *Cold Spring Harbor Perspectives in Medicine*. 2018; 8: a029686.
- [2] Seebacher F. Responses to temperature variation: integration of thermoregulation and metabolism in vertebrates. *Journal of Experimental Biology*. 2009; 212: 2885–2891.
- [3] Burch N, Arnold A, Item F, Summermatter S, Brochmann Santana Santos G, Christe M, *et al*. Electric pulse stimulation of cultured murine muscle cells reproduces gene expression changes of trained mouse muscle. *PLoS ONE*. 2010; 5: e10970.
- [4] Marek-Iannucci S, Thomas A, Hou J, Crupi A, Sin J, Taylor DJ, *et al*. Myocardial hypothermia increases autophagic flux, mitochondrial mass and myocardial function after ischemia-reperfusion injury. *Scientific Reports*. 2019; 9: 10001.
- [5] Wright GL, Maroulakou IG, Eldridge J, Liby TL, Sridharan V, Tsiachlis PN, *et al*. VEGF stimulation of mitochondrial biogenesis: requirement of AKT3 kinase. *FASEB Journal*. 2008; 22: 3264–3275.
- [6] Miranda S, Foncea R, Guerrero J, Leighton F. Oxidative stress and upregulation of mitochondrial biogenesis genes in mitochondrial DNA-depleted HeLa cells. *Biochemical and Biophysical Research Communications*. 1999; 258: 44–49.
- [7] Heddi A, Stepien G, Benke PJ, Wallace DC. Coordinate induction of energy gene expression in tissues of mitochondrial disease patients. *Journal of Biological Chemistry*. 1999; 274: 22968–22976.
- [8] Bhowmick S, Drew KL. Mechanisms of innate preconditioning towards ischemia/anoxia tolerance: Lessons from mammalian hibernators. *Conditioning Medicine*. 2019; 2: 134–141.
- [9] Durukan A, Tatlisumak T. Preconditioning-induced ischemic tolerance: a window into endogenous gearing for cerebroprotection. *Experimental and Translational Stroke Medicine*. 2010; 2: 2.
- [10] Yang T, Li Q, Zhang F. Regulation of gene expression in ischemic preconditioning in the brain. *Conditioning Medicine*. 2017; 1: 47–56.



- [11] Greene LA, Tischler AS. Establishment of a noradrenergic clonal line of rat adrenal pheochromocytoma cells which respond to nerve growth factor. *Proceedings of the National Academy of Sciences USA*. 1976; 73: 2424–2428.
- [12] Westerink RH, Ewing AG. The PC12 cell as model for neurosecretion. *Acta Physiologica*. 2008; 192: 273–285.
- [13] Sandhu JK, Pandey S, Ribecco-Lutkiewicz M, Monette R, Borowy-Borowski H, Walker PR, *et al.* Molecular mechanisms of glutamate neurotoxicity in mixed cultures of NT2-derived neurons and astrocytes: Protective effects of coenzyme Q10. *Journal of Neuroscience Research*. 2003; 72: 691–703.
- [14] Byrd AS, Sikorska M, Walker PR, Sandhu JK. Effects of glutathione depletion on the viability of human NT2-derived neuronal and astroglial cultures. *Neuron Glia Biology*. 2004; 1: 317–326.
- [15] Sikorska M, Sandhu JK, Deb-Rinker P, Jezierski A, Leblanc J, Charlebois C, *et al.* Epigenetic modifications of SOX2 enhancers, SRR1 and SRR2, correlate with in vitro neural differentiation. *Journal of Neuroscience Research*. 2008; 86: 1680–1693.
- [16] Kondziolka D, Steinberg GK, Cullen SB, McGrogan M. Evaluation of surgical techniques for neuronal cell transplantation used in patients with stroke. *Cell Transplantation*. 2004; 13: 749–754.
- [17] Keefer LK, Nims RW, Davies KM, Wink DA. “NONOates” (1-substituted diazen-1-ium-1,2-diols) as nitric oxide donors: Convenient nitric oxide dosage forms. *Methods in Enzymology*. 1996; 82: 281–293.
- [18] Borowy-Borowski H, Sodja C, Docherty J, Walker PR, Sikorska M. Unique technology for solubilization and delivery of highly lipophilic bioactive molecules. *Journal of Drug Targeting*. 2004; 12: 415–424.
- [19] Sikorska M, Borowy-Borowski H, Zurakowski B, Walker PR. Derivatised alpha-tocopherol as a CoQ10 carrier in a novel water-soluble formulation. *BioFactors*. 2003; 18: 173–183.
- [20] Sandhu JK, Sodja C, McRae K, Li Y, Rippstein P, Wei YH, *et al.* Effects of nitric oxide donors on cybrids harbouring the mitochondrial myopathy, encephalopathy, lactic acidosis and stroke-like episodes (MELAS) a3243G mitochondrial DNA mutation. *The Biochemical Journal*. 2005; 391: 191–202.
- [21] Costain WJ, Rasquinha I, Sandhu JK, Rippstein P, Zurakowski B, Slinn J, *et al.* Cerebral ischemia causes dysregulation of synaptic adhesion in mouse synaptosomes. *Journal of Cerebral Blood Flow and Metabolism*. 2008; 28: 99–110.
- [22] Essop MF. Cardiac metabolic adaptations in response to chronic hypoxia. *The Journal of Physiology*. 2007; 584: 715–726.
- [23] Ventura-Clapier R, Garnier A, Veksler V. Transcriptional control of mitochondrial biogenesis: the central role of PGC-1 $\alpha$ . *Cardiovascular research*. 2008; 79: 208–217.
- [24] Tasca CI, Dal-Cim T, Cimarosti H. In vitro oxygen-glucose deprivation to study ischemic cell death. *Methods in Molecular Biology*. 2015; 1254: 197–210.
- [25] Finkel T. Signal transduction by reactive oxygen species. *The Journal of Cell Biology*. 2011; 194: 7–15.
- [26] Pleasure SJ, Lee VM. NTER 2 cells: A human cell line which displays characteristics expected of a human committed neuronal progenitor cell. *Journal of Neuroscience Research*. 1993; 35: 585–602.
- [27] Berman SB, Pineda FJ, Hardwick JM. Mitochondrial fission and fusion dynamics: the long and short of it. *Cell Death and Differentiation*. 2008; 15: 1147–1152.
- [28] Sharp FR, Ran R, Lu A, Tang Y, Strauss KI, Glass T, *et al.* Hypoxic preconditioning protects against ischemic brain injury. *NeuroRx*. 2004; 1: 26–35.
- [29] Wang L, Wang A, Guo H, Zhang Z, Wang S, Pei T, *et al.* Neuroprotective effects of long-term metformin preconditioning on rats with ischemic brain injuries. *European Neurology*. 2021; 84: 212–218.
- [30] Stetler RA, Leak RK, Yin W, Zhang L, Wang S, Gao Y, *et al.* Mitochondrial biogenesis contributes to ischemic neuroprotection afforded by LPS pre-conditioning. *Journal of Neurochemistry*. 2012; 123: 125–137.
- [31] Gutsaeva DR, Carraway MS, Suliman HB, Demchenko IT, Shitara H, Yonekawa H, *et al.* Transient hypoxia stimulates mitochondrial biogenesis in brain subcortex by a neuronal nitric oxide synthase-dependent mechanism. *The Journal of Neuroscience*. 2008; 28: 2015–2024.
- [32] Torosyan R, Huang S, Bommi PV, Tiwari R, An SY, Schonfeld M, *et al.* Hypoxic preconditioning protects against ischemic kidney injury through the IDO1/kynurenine pathway. *Cell Reports*. 2021; 36: 109547.
- [33] Vayssière JL, Cordeau-Lossouarn L, Larcher JC, Basseville M, Gros F, Croizat B. Participation of the mitochondrial genome in the differentiation of neuroblastoma cells. *In Vitro Cellular and Developmental Biology*. 1992; 28A: 763–772.
- [34] Dominy JE, Puigserver P. Mitochondrial biogenesis through activation of nuclear signaling proteins. *Cold Spring Harbor Perspectives in Biology*. 2013; 5: a015008.
- [35] Bouchez C, Devin A. Mitochondrial biogenesis and mitochondrial reactive oxygen species (ROS): A complex relationship regulated by the cAMP/PKA signaling pathway. *Cells*. 2019; 8: 287.
- [36] Roczek CR, Chandel NS. ROS-dependent signal transduction. *Current Opinion in Cell Biology*. 2015; 33: 8–13.
- [37] Gáspár T, Kis B, Snipes JA, Lenzser G, Mayanagi K, Bari F, *et al.* Neuronal preconditioning with the antianginal drug, bepridil. *Journal of Neurochemistry*. 2007; 102: 595–608.
- [38] Sun JZ, Tang XL, Park SW, Qiu Y, Turrens JF, Bolli R. Evidence for an essential role of reactive oxygen species in the genesis of late preconditioning against myocardial stunning in conscious pigs. *The Journal of Clinical Investigation*. 1996; 97: 562–576.
- [39] Wakabayashi N, Slocum SL, Skoko JJ, Shin S, Kensler TW. When NRF2 talks, who’s listening? *Antioxidants and Redox Signaling*. 2010; 13: 1649–1663.
- [40] Cao YJ, Shibata T, Rainov NG. Hypoxia-inducible transgene expression in differentiated human NT2N neurons—a cell culture model for gene therapy of postischemic neuronal loss. *Gene Therapy*. 2001; 8: 1357–1362.
- [41] Lee HC, Wei YH. Mitochondrial biogenesis and mitochondrial DNA maintenance of mammalian cells under oxidative stress. *The International Journal of Biochemistry and Cell Biology*. 2005; 37: 822–834.
- [42] Wu SB, Wei YH. AMPK-mediated increase of glycolysis as an adaptive response to oxidative stress in human cells: implication of the cell survival in mitochondrial diseases. *Biochimica et Biophysica Acta-Molecular Basis of Disease*. 2012; 1822: 233–247.
- [43] Wilson JE. Isozymes of mammalian hexokinase: structure, subcellular localization and metabolic function. *The Journal of Experimental Biology*. 2003; 206: 2049–2057.
- [44] Timón-Gómez A, Nývltová E, Abriata LA, Vila AJ, Hosler J, Barrientos A. Mitochondrial cytochrome c oxidase biogenesis: Recent developments. *Seminars in Cell and Developmental Biology*. 2018; 76: 163–178.
- [45] Gureev AP, Shafarostova EA, Popov VN. Regulation of mitochondrial biogenesis as a way for active longevity: interaction between the Nrf2 and PGC-1 $\alpha$  signaling pathways. *Frontiers in Genetics*. 2019; 10: 435.
- [46] Piantadosi CA, Carraway MS, Babiker A, Suliman HB. Heme oxygenase-1 regulates cardiac mitochondrial biogenesis via Nrf2-mediated transcriptional control of nuclear respiratory factor-1. *Circulation Research*. 2008; 103: 1232–1240.
- [47] Horbay R, Bilyy R. Mitochondrial dynamics during cell cycling.

- Apoptosis. 2016; 21: 1327–1335.
- [48] Chacinska A, Koehler CM, Milenkovic D, Lithgow T, Pfanner N. Importing mitochondrial proteins: Machineries and mechanisms. *Cell*. 2009; 138: 628–644.
  - [49] Cam H, Balciunaite E, Blais A, Spektor A, Scarpulla RC, Young R, *et al.* A common set of gene regulatory networks links metabolism and growth inhibition. *Molecular Cell*. 2004; 16: 399–411.
  - [50] Cooper DJ, Walter CA, McCarrey JR. Co-regulation of pluripotency and genetic integrity at the genomic level. *Stem Cell Research*. 2014; 13: 508–519.
  - [51] Wang L, Wang R, Herrup K. E2F1 works as a cell cycle suppressor in mature neurons. *The Journal of Neuroscience*. 2007; 27: 12555–12564.
  - [52] Parrales A, López E, Lee-Rivera I, López-Colomé AM. ERK1/2-dependent activation of mTOR/mTORC1/p70S6K regulates thrombin-induced RPE cell proliferation. *Cellular Signaling*. 2013; 25: 829–838.
  - [53] Ino H, Chiba T. Cyclin-dependent kinase 4 and cyclin D1 are required for excitotoxin-induced neuronal cell death in vivo. *The Journal of Neuroscience*. 2001; 21: 6086–6094.
  - [54] Herrup K, Yang Y. Cell cycle regulation in the postmitotic neuron: oxymoron or new biology? *Nature Reviews Neuroscience*. 2007; 8: 368–378.
  - [55] Valero T. Mitochondrial biogenesis: pharmacological approaches. *Current Pharmaceutical Design*. 2014; 20: 5507–5509.
  - [56] Simmons EC, Scholpa NE, Schnellmann RG. Mitochondrial biogenesis as a therapeutic target for traumatic and neurodegenerative CNS diseases. *Experimental Neurology*. 2020; 329: 113309.